Electronic transport behaviors of Ni-Nb-Zr-H glassy alloys

doi: 10.1063/1.3284207

Electronic transport behaviors of Ni–Nb–Zr–H glassy alloys

M. Fukuhara,[1,a] H. Yoshida,[1] K. Koyama,[1] A. Inoue,[2] and Y. Miura[3]
[1]*Institute for Materials Research, Tohoku University, Sendai 980-8577, Japan*
[2]*Tohoku University, Sendai 980-8577, Japan*
[3]*Research Institute of Electrical Communication, Tohoku University, Sendai 980-8577, Japan*

(Received 24 August 2009; accepted 5 December 2009; published online 1 February 2010)

The electronic transport behaviors of $(Ni_{0.36}Nb_{0.24}Zr_{0.40})_{100-y}H_y$ $(0 \le y \le 20)$ glassy alloys with distorted nanostructural icosahedral $Zr_5Nb_5Ni_3$ clusters have been studied as a function of hydrogen content. These alloys show semiconducting, room-temperature superior electric transport, superconducting (onset temperature of 10 K) and electron avalanche behaviors, and electric current-induced voltage (Coulomb) oscillation, as hydrogen content increases. These results suggest that the localization effect of hydrogen at the outside and inside space of the clusters plays important roles in various electron transport phenomena. © *2010 American Institute of Physics*.
[doi:10.1063/1.3284207]

I. INTRODUCTION

Glassy alloys are peculiar metallic alloys that lack the long-range cyclic order of crystalline alloys, on the nanoscale.[1,2] Therefore, glassy alloys, which are considered to be a macroscopic material with a mesoscopic system of nanostructures, are candidate materials for future nanoelectronic devices. Following the theoretical pioneering work of Ben–Jacob and Grefen[3] and the subsequent discovery of the Coulomb blockade effect by quantum-dot tunneling at low temperature,[4,5] especially, a number of studies have reported to achieve room-temperature oscillation.[6–11] Recently, we observed electric current-induced voltage oscillation in $[(Ni_{0.6}Nb_{0.4})_{1-x}Zr_x]_{1-y}H_y$ $(30 \le x \le 50,\ 0 \le y \le 0.2)$,[12–14] $[(Ni_{0.6}Nb_{0.4})_{1-s}Zr_s]_{1-z}D_z$ $(s=0.30,\ 0.35,\ 0.40,$ and $0.45,$ $0.091 \le z \le 0.148)$,[15] and $(Ti_{0.5}Ni_{0.25}Cu_{0.25})_{1-t}H_t (0 \le t \le 0.152)$ (Ref. 16) glassyalloys with multiple junctions in the temperature range of 373–6 K, based on Coulombic oscillation of protons (deuteron). We propose the tunnelling of individual protons that are charging and discharging the vacancy capacitance of Zr-H(D)-□-H(D)-Zr atomic bond arrays among the Zr(Nb)-tetrahedral sites, where □ is the vacancy barrier, termed the free volume, in the glassy alloys. Furthermore, the frequency of the $(Ni_{36}Nb_{24}Zr_{40})_{90.1}H_{9.9}$ glassy alloy decreased remarkably with increasing capacitance (C) and resistance (R) in the dc/ac circuit at room temperature.[14] This resembles discharging behavior in which a constant voltage-discharge tube with a parallel condenser and high resistance causes block oscillation, which is derived from the charging and discharging of the capacitance.[17] Thus the glassy alloy could be regarded as a dc/ac converting device with a large number of nanofarad capacitance.[14] Indeed, the hydrogenated glassy alloy is characterized by an assembly (free volume) of such vacancies (0.7–3 at. %),[18] which are distributed homogeneously among the icosahedral clusters. This is in sharp contrast to crystalline alloys with higher hydrogen content, in which cooperative motions of hydrogen are present.[19] Furthermore, the hydrogen atoms of Ni–Nb–Zr glassy alloys settle stably into four-coordination sites that are surrounded tetrahedrally by four Zr(Nb) atoms.[20]

In this study, we report on the various electronic transport behaviors, in addition to Coulombic oscillation, of individual Ni–Nb–Zr–H glassy alloys. We have chosen a melt-spun flexible amorphous alloy $[(Ni_{0.6}Nb_{0.4})_{1-x}Zr_x]_{1-y}H_y$ (x $=0.30,$ 0.32, 0.34, 0.35, 0.36, 0.38, 0.40, 0.45, and 0.50, $0 \le y \le 0.20$) with excellent hydrogen permeability,[21] as the matrix specimen. The alloy is a typical metal-metal-type alloy that consists of familiar transition elements. Our interest lies in investigating the hydrogen-dependent electronic transport behaviors of the $(Ni_{0.36}Nb_{0.24}Zr_{0.40})_{100-y}H_y$ $(0 \le y \le 20)$ glassy alloys in terms of localization effect of hydrogen. However, these are no previous reports on this subject for glassy alloys with hydrogen.

II. EXPERIMENTAL

The rotating wheel method under an argon atmosphere was used for the preparation from argon arc-melted ingots of amorphous $[(Ni_{0.6}Nb_{0.4})_{1-x}Zr_x]_{1-y}H_y$ alloy ribbons of 1-mm width and 20-μm thickness. Hydrogen charging was carried out electrolytically in 0.5 M H_2SO_4 and 1.4 g/L thiourea (H_2NCSNH_2) at room temperature and current densities of 30 A/m^2.[22]

The specific electrical resistances of hydrogenated specimens were measured by the four-probe method.[12–16] The current-voltage (I-V) curve for the four-probe method was measured from 0 to 100 mA with a constant current step of ± 0.1 mA at room temperature, using Semiconductor Characterization System 4200 (Keithley Instruments Inc.). Electrical resistance measurements of onset superconductivity were determined by the temperature dependence of the dc current four-probe method at a cooling rate of 1 K/min from 323 to 4.2 K in He of ambient pressure under a magnetic in the High Field Laboratory (IMR, Tohoku University).

The optional atom configuration and the adiabatic potential energy curve of the icosahedral cluster that consisted of Ni–Nb–Zr–H were calculated by the first-principles density

[a]Author to whom correspondence should be addressed. Electronic mail: fukuhara@imr.tohoku.ac.jp.

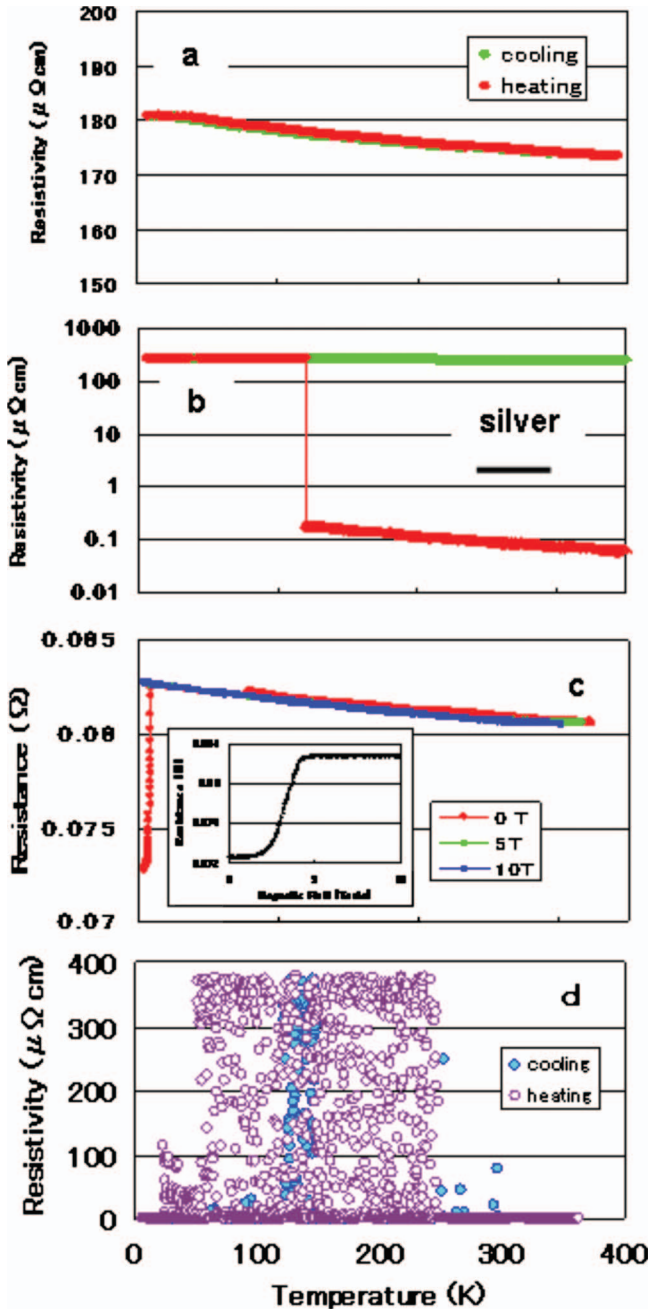

FIG. 1. (Color) Temperature dependence of the resistivities of the $(Ni_{0.36}Nb_{0.24}Zr_{0.40})_{100-y}H_y$ alloys with different hydrogen contents (a) ($y=0$), semiconducting; (b) ($y=3.9$), superior conducting; (c) ($y=5.7$), superconducting transports; and (d) ($y=9.3$), Coulombic oscillation.

functional calculations using the VIENNA *AB INITIO SIMULATION PACKAGE*.[23] The nuclei and core electrons are described by the projector augmented plane-wave method[24] and the wave functions are expanded in a plane wave basis set with a cut-off energy of 293.2 eV.

III. RESULTS

A. Effect of hydrogen for various electronic behaviors

The temperature dependencies of the resistivities of $(Ni_{0.36}Nb_{0.24}Zr_{0.40})_{100-y}H_y$ ($0 \le y \le 20$) glassy alloys with different hydrogen contents are shown in Fig. 1. The resistivities showed large differences with increasing hydrogen content [Figs. 1(a)–1(d)]. The resistivity of $Ni_{36}Nb_{24}Zr_{40}$, which lacks hydrogen, increased almost linearly with decreasing temperature down to 6 K [Fig. 1(a)]. The negative temperature coefficient of resistivity (TCR) value of -12.18×10^{-5}/K indicates a semiconducting character.

The resistivity of the $(Ni_{0.36}Nb_{0.24}Zr_{0.40})_{96.1}H_{3.9}$ alloy initially showed negative TCR behavior similar to the alloy without hydrogen in the cooling run. However, in the heating run, the resistivity decreased up to 123 K according to the same curve as the cooling run but suddenly decreased to 3rd order [Fig. 1(b)] at 124 K and then descended with TCR of -7.55×10^{-3}/K up to 350 K. The resistivity (0.07 $\mu\Omega$ cm) at 300 K was one-twentieth that of silver (1.62 $\mu\Omega$ cm) at room temperature. The similar behaviors were also intensively observed for the $(Ni_{0.39}Nb_{0.26}Zr_{0.35})_{100-y}H_y$ ($y=5.6$, 6.3, 7, and 7.5) and $(Ni_{0.396}Nb_{0.264}Zr_{0.34})_{100-y}H_y$ ($y=6.2$ and 7.9) alloys. This superior conductivity resembles the ballistic transport observed in one-dimensional, nanometer-scale channels, such as quantum wires[25] and carbon nanotubes[26,27] at low temperature, in the form of quantum interference associated with coherence. However, it is not clear at present time whether the mean free path of the electron is much greater than the size of the medium or not. Thus, room-temperature, superior transport behavior at the millimeter-size level is of interest not only for the development of electronic devices but also for electric power applications. As regards the cause of the drop in resistivity at 124 K, although topologic change (pseudotransition) associated with the accumulation of strain is a possibility,[28] we cannot confirm this without further investigation.

The resistivity of the $(Ni_{0.36}Nb_{0.24}Zr_{0.40})_{94.3}H_{5.7}$ alloy increased with TCR of -7.05×10^{-5}/K down to 9.5 K and then plunged to a dive down to 4.2 K [Fig. 1(c)]. However the resistivity continued without decrease to 4.2 K under magnetic fields of 5 and 10 T. Indeed, the application of a magnetic field >4.7 T arrested the drop of resistivity [see inset in Fig. 1(c)]. Thus, the drop from 9.5 K suggests the existence of superconductivity of type II. The detailed results for diamagnetic effect will be described in a subsequent paper.[29] Hydrogen of the distorted icosahedral Zr–Nb–Ni cluster expands the Zr(Nb) tetrahedral sites,[30,31] leading to a decrement in the atomic distances of the neighboring sites due to the high-pressure effect of hydrogen. Since the cluster can be regarded as a nanoscopic (~1 nm) metallic island that is isolated from other islands by potential barriers in the sub-nanometer range, the tunneling of electron pairs to allow transport among the clusters is feasible.

Figure 1(d) shows the temperature-dependent electric resistivity of a $(Ni_{0.36}Nb_{0.24}Zr_{0.40})_{90.7}H_{9.3}$ alloy. The abnormal resistivity continued from 148 K down to 127 K in the cooling run and from 27 K to up to 245 K in the heating run. This is the electric current-induced voltage amplification based on Coulombic oscillation of a proton, as described above. However, when the glassy alloy absorbed hydrogen over a threshold content, the point at which hydrogen atoms fully occupied the tetrahedral sites that are surrounded in a tetrahedral arrangement by four Zr(Nb) atoms, the hydrogen was forced to penetrate into the vacancies and consequently, the tunnel-

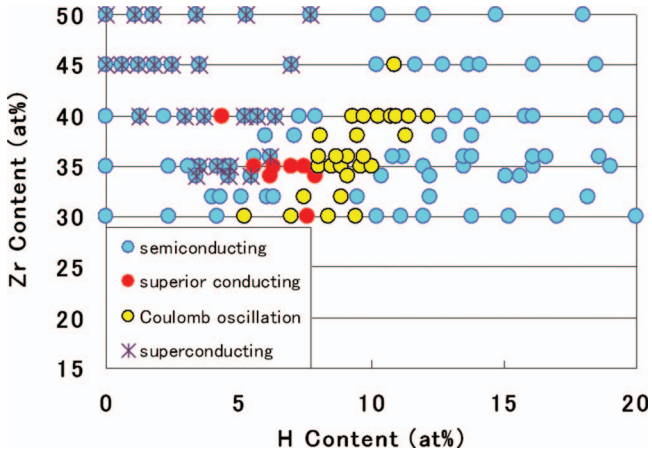

FIG. 2. (Color) The effects of Zr and H contents on the occurrence of semiconducting, superior conducting, and superconducting transport and Coulombic oscillation properties of the $[(Ni_{0.6}Nb_{0.4})_{1-x}Zr_x]_{1-y}H_y$ $(30 \leq x \leq 50,\ 0 \leq y \leq 0.2)$ glassy alloys.

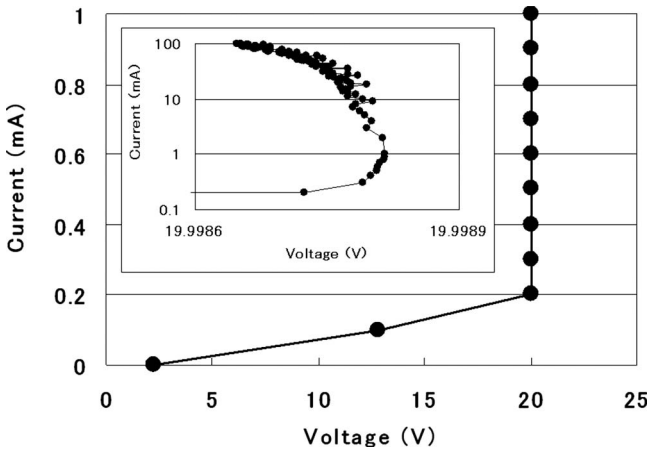

FIG. 3. *I-V* characteristic of the $(Ni_{0.36}Nb_{0.24}Zr_{0.40})_{90.1}H_{9.9}$ glassy alloy at room temperature.

ing phenomenon disappeared. Thus, the Coulombic oscillation of the proton requires an appropriate atomic ratio of Zr to hydrogen (Zr:H) of 4:1.

We observed similar resistivity variations for restricted contents of hydrogen and Zr. The effects of Zr and H content on these variations for $[(Ni_{0.6}Nb_{0.4})_{1-x}Zr_x]_{1-y}H_y$ glassy alloys are collectively presented in Fig. 2. In the figure, the blue, red, and green solids represent the alloys that were observed to have semi- and superior conducting properties and Coulombic dot tunneling, respectively, and the cross denotes alloys that showed onset superconductivity above 5.5 K. The electronic transport behaviors of interest can be classified into four groups. Since superior electric transport occurs at limited region of 34–35 at. % Zr and 5–7.5 at. % H, the representative example for the alloy with 35 at. % Zr is presented at Fig. 5 in Appendix.

B. Negative resistance

In reference [14], the frequency of Coulombic oscillation decreased remarkably with increasing capacitance and resistance at room temperature. This behavior is analogous to block oscillation with charge-discharge in a discharge tube. The oscillation in the discharge tube replaces a semiconductor with negative resistance.[32] Negative resistance is a property of electrical circuit elements that are composed of certain materials for which, over certain voltage ranges, current is a decreasing function of voltage. There are two forms of negative resistance, type *N* and type *S*. The former, which shows voltage-controlled behavior, is used in devices such as the tunnel diode and Gunn diode, while the latter current-controlled type is found in devices such as the unijunction transistor, neon lamps, thyristors, resonant tunneling transistors, and old carbon arc oscillators.

We measured the current-controlled *I-V* characteristics of the $(Ni_{36}Nb_{24}Zr_{40})_{90.1}H_{9.9}$ alloy in the current region from 0 to 100 mA (Fig. 3). The current did not flow up to 2.24 V, irrespective of voltage, and then increased linearly up to 19.99 V under the Ohmic rule. Subsequently, the current jumped to 100 mA, reflecting an electron avalanche. Strictly speaking, the voltage was reduced slightly at high-current (inset in Fig. 3). Thus, it is clear that the glassy alloy is transformed suddenly from an insulator into an extremely good conductor. This behavior resembles that of a current-controlled *S* type negative resistor. Although it is known that there are high- and low-current density regions in a region of negative resistance, we could not measure the electrical characteristics of the high-current-density region owing to the high-density limitation of our device.

IV. DISCUSSION

As can be seen from above mentioned results, the doping of hydrogen for glassy alloys of interest plays important roles in various electron transport phenomena. We consider the reason the calculated adiabatic potential energy of the hydrogen atom for the distorted icosahedral $Zr_5Ni_5Nb_3$ cluster, with composition close to that of the $Ni_{36}Nb_{24}Zr_{40}$ alloy, provided that the energy of the hydrogen on the surface of cluster is not significantly changed by the presence of the nearly cluster. The potential energy (A in Fig. 4) of hydrogen adsorbed by the outer surface of the cluster was lower than that (B in Fig. 4) of the bonding state between Zr (or Nb) and H atoms settled in the cluster. In other words, the outer adsorbed hydrogen of the cluster is in a stable state and the inner bonding hydrogen in the tetrahedral is in a metastable state. This result provides the following assumptions. The hydrogen atom localizes to a space site between the clusters and then enlarges the space and lastly construct zigzag tunnels of width 0.26 nm on average (the width will be reported in coming-up paper[33]) due to high pressure effect of hydrogen in electroanalysis, as hydrogen content increases. When hydrogen content reaches to around 7 at. %, the hydrogen begins to plunge into the tetrahedral sites of the clusters. However, since the clusters are combined with small amount of the Voronoi-type polyhedra, precise calculation needs detailed information for atomic configuration.

The localization of hydrogen also induces shrinkage of atomic distance in addition to construction of tunnels, as reported in previous papers.[30,31] Thus, the existence of the outer hydrogen appears to be related to the occurrence of superior electric transport. In this case, the superior conduc-

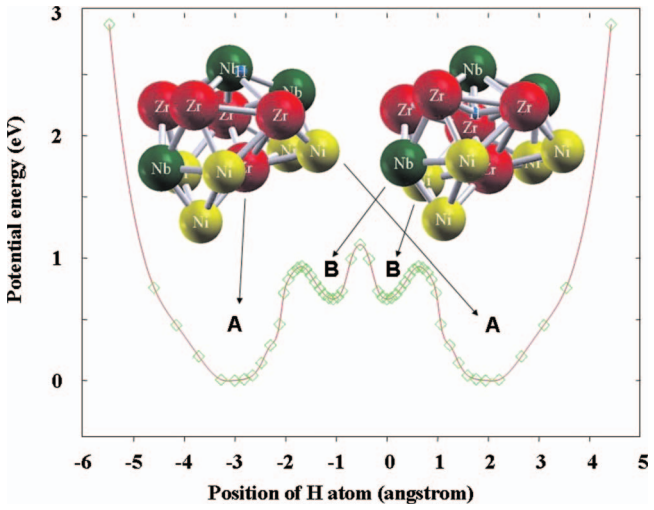

FIG. 4. (Color) Calculated potential energy curve for the interaction of the H atom with the icosahedral $Zr_5Ni_5Nb_3$ cluster as a function of the position of the H atom relative to the cluster. The models comprise $Zr_5Ni_5Nb_3$ clusters with hydrogen adsorbed to the outer front of the cluster and combined with Zr(Nb) atoms in the cluster.

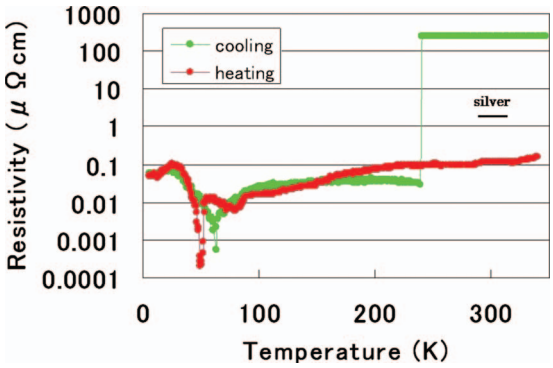

FIG. 5. (Color) Superior conducting behavior of the $(Ni_{0.39}Nb_{0.26}Zr_{0.35})_{93.7}H_{6.3}$ alloy.

tance would be derived from electron tunneling along the cluster arrays because the mean free path of the electron is larger than that (~0.26 nm) (Ref. 33) of the tunnel width between clusters. Indeed, the electrical transport in multiwalled carbon nanotubes is shown to be ballistic at room temperature with mean free paths on the order of tens of microns.[27] Since the glassy alloy can be considered as a self-organized assembly of low-capacitance, multiple-junction configurations, *i.e.*, a huge assembly of 1-nm-sized quantum dots, by ac impedance analyses,[33] we can image the existence of macroscopic quantum electron tunneling passes along the arrays in the glassy alloys, even if there are poor conduction cluster passes combined with small amounts of other Voronoi-type polyhedra with relatively long atomic distances.[33,34] The superior conductance effect is promising for future electron devices and electric power applications such as lower supply voltage and leading to low power consumption. Further work in this interesting area based on cluster science is warranted. Furthermore, the atomic configuration for the icosahedral clusters shown in Fig. 4 becomes stable when the number of Ni atom is 4–5 in an icosahedral cluster consisting of 13 atoms.

In contrast, superconductivity occurred with hydrogen compositions of 0–8 at. %. The atomic configurations of $Ni_{36}Nb_{24}Zr_{40}$ and $(Ni_{36}Nb_{24}Zr_{40})_{90.1}H_{9.9}$ glassy alloys have been analyzed by x-ray absorption of fine structure (XAFS) measurement using strong radiation photos of SPring-8.[30,31] The atomic radii of Zr, Nb and Ni (0.1655, 0.1605, and 0.0985, respectively) for $(Ni_{36}Nb_{24}Zr_{40})_{90.1}H_{9.9}$ glassy alloy are longer than those of crystalline Zr and Nb, and shorter than one of crystalline Ni, in comparison with those of the crystalline forms (0.160, 0.145, and 0.124 nm, respectively).[35] The shorter atomic distance is necessary and sufficient for the occurrence of superconductivity.[29,36] Based on the atomic configuration of the Zr–Ni–Al system,[37] we can postulate millimeter-size zigzag paths linking the Ni–Ni–Ni-array in the distorted icosahedral Zr–Nb–Ni clusters to the array in the neighbor one, by electron pair tunneling. It is known that the electron pair, as well as a single electron, could easily tunnel between the clusters with size of 1 nm. Thus the cluster can be also regarded as a nanoscopic (~1 nm) metallic island that is isolated from other islands by potential barriers of vacancy. In addition, destruction of superconductivity could be derived from electromagnetic repulsion between Ni spins in the cluster or between Ni spin in the cluster and Ni one in the neighbor cluster under strong magnetic field, leading to total orbital angular magnetic moment, $L \neq 0$.[29,38]

The drop in resistivity at 124 K in heating run of Fig. 1(b) and at 240 K in cooling run of Fig. 5 (see Appendix) would be due to topologic change (pseudotransition) of clusters, as well as a cause of internal friction peaks in low temperature regions.[28] The morphology change is associated with two kinds of cluster ordering.[39] One is due to the special short range ordering, so-called topological short range ordering, and another is the chemical short range ordering, so-called compositional short range ordering. The intrinsic cause of the drop in resistivity needs for precise atomic configuration analysis. Furthermore, it is difficult to elucidate the cause of valleys at 63 and 51 K in cooling and heating runs of Fig. 5, respectively, at present time. In this interesting work, it requires further studies such as measurement and theory of mean free path of electrons.

V. CONCLUSIONS

Characteristic electric resistivity of the $(Ni_{0.36}Nb_{0.24}Zr_{0.40})_{100-y}H_y$ $(0 \leq y \leq 20)$ glassy alloys with distorted nanostructural icosahedral $Zr_5Nb_5Ni_3$ clusters was measured in the temperature region between 373 and 6 K. The resistivity of alloy without hydrogen showed semiconducting behavior. The $(Ni_{0.36}Nb_{0.24}Zr_{0.40})_{96.1}H_{3.9}$ alloy revealed superior electric transport which was one-twentieth lowers than resistivity of silver at room temperature. The resistivity measurement of the $(Ni_{0.36}Nb_{0.24}Zr_{0.40})_{94.3}H_{5.7}$ alloy showed a type II-superconductivity with onset temperature of 10 K, but the application of a magnetic field >4.7 T arrested the drop of resistivity. The resistivity of the $(Ni_{0.36}Nb_{0.24}Zr_{0.40})_{90.7}H_{9.3}$ and the $(Ni_{0.36}Nb_{0.24}Zr_{0.40})_{90.1}H_{9.9}$ alloys showed the electric current-induced voltage (Coulomb) oscillation and the electron avalanche behavior ob-

served in current-controlled *S* type negative resistor, respectively. From the calculated adiabatic potential energy of the hydrogen atom for the distorted icosahedral $Zr_5Ni_5Nb_3$ cluster, these results suggest that the localization effect of hydrogen at the outside and inside space of the clusters plays important roles in various electron transport phenomena. Thus this paper will throw new light for new science and technologies based on cluster science.

ACKNOWLEDGMENTS

This work was supported by a Grant-In-Aid for Science Research in the priority Area "Research and Development Project on Advanced Metallic Glasses, Inorganic Materials, and Joining Technology" from the Ministry of Education, Science, Sports, and Culture, Japan.

APPENDIX

Although hydrogen effect-electronic transport behaviors for the $(Ni_{0.36}Nb_{0.24}Zr_{0.40})_{100-y}H_y$ $(0 \leq y \leq 20)$ glassy alloys were reported in Figs. 1 and 4, the similar behaviors were also observed in other compositions, as shown in Fig. 2. The superior conducting behaviors were also intensively observed for the $(Ni_{0.39}Nb_{0.26}Zr_{0.35})_{100-y}H_y$ ($y=5.6$, 6.3, 7, and 7.5) and $(Ni_{0.396}Nb_{0.264}Zr_{0.34})_{100-y}H_y$ ($y=6.2$ and 7.9) alloys. We show the representative data for the alloy with 35 at. % Zr, $(Ni_{0.39}Nb_{0.26}Zr_{0.35})_{93.7}H_{6.3}$, in Fig. 5, to make assurance doubly sure. The resistivity of the $(Ni_{0.39}Nb_{0.26}Zr_{0.35})_{93.7}H_{6.3}$ suddenly falls down to order of 0.01 $\mu\Omega$ cm at 240 K, and then continued down to around 100 K in cooling run. Subsequently the resistance showed one valley at 63 K, and lastly recovered to order of 0.01 $\mu\Omega$ cm as the temperature decreased. In the heating run, the resistivity varied according to the similar curve as the cooling run, except for minimum value at 51 K, and then ascended once again as the temperature increased to 341 K. The resistivity (0.12 $\mu\Omega$ cm) at 300 K was one-fourteenth that of silver (1.62 $\mu\Omega$ cm) at room temperature.

[1]G. J. Fan and H. J. Fecht, J. Chem. Phys. **116**, 5002 (2002).
[2]A. R. Yavari, Nature (London) **439**, 405 (2006).
[3]E. Ben-Jacob and Y. Grefen, Phys. Lett. **108A**, 289 (1985).
[4]M. A. Kastner, P. F. Kwasnick, and J. C. Licini, Phys. Rev. B **36**, 8015 (1987).
[5]T. A. Fulton and G. J. Dolan, Phys. Rev. Lett. **59**, 109 (1987).
[6]K. Yano, T. Ishi, T. Hashimoto, T. Kobayashi, and F. Murai, IEEE Trans. Electron Devices **41**, 1628 (1994).
[7]H. Ishikuro, T. Fujii, T. Saraya, G. Hashiguchi, T. Hiramoto, and T. Ikoma, Appl. Phys. Lett. **68**, 3585 (1996).
[8]L. Guo, E. Leobandung, and S. Y. Chou, Science **275**, 649 (1997).
[9]S. J. Tans, A. R. M. Verschueren, and C. Dekker, Nature (London) **393**, 49 (1998).
[10]R. Martel, T. Schmidt, H. R. Shea, T. Hertel, and Ph. Avouris, Appl. Phys. Lett. **73**, 2447 (1998).
[11]H. W. Ch. Postma, T. Teepen, Z. Yao, M. Grifoni, and C. Dekke, Science **293**, 76 (2001).
[12]M. Fukuhara, A. Kawashima, S. Yamaura, and A. Inoue, Appl. Phys. Lett. **90**, 203111 (2007).
[13]M. Fukuhara, S. Yamaura, and A. Inoue, J. Phys.: Conf. Ser. **144**, 012086 (2009).
[14]M. Fukuhara and A. Inoue, J. Appl. Phys. **105**, 063715 (2009).
[15]M. Fukuhara and A. Inoue, Europhys. Lett. **83**, 36002 (2008).
[16]M. Fukuhara, S. Yamaura, and A. Inoue, Phys. Status Solidi B **246**, 153 (2009)
[17]M. H. Jones, *A Practical Introduction to Electronic Circuits*, 3rd ed. (Cambridge University Press, Cambridge, 1995), p. 654.
[18]S. Yamaura, H. M. Kimura, A. Inoue, M. Nishida, Y. Shinpo, and H. Okuchi, Trans. Mater. Res. Soc. Jpn. **29**, 3251 (2004).
[19]M. Fukuhara, Acoust. Lett. **23**, 60 (1999).
[20]M. Fukuhara, A. Kawashima, S. Yamaura, and A. Inoue, Phys. Status Solidi **1**, R50 (2007).
[21]S. Yamaura, M. Sakurai, M. Hasegawa, K. Wakoh, Y. Shimpo, M. Nishida, H. Kimura, E. Matsubara, and A. Inoue, Acta Mater. **53**, 3703 (2005).
[22]A. Kawashima, S. Yamaura, N. Ohtsu, H. Kimura, and A. Inoue, Mater. Trans. **47**, 1523 (2006).
[23]G. Kresse and J. Furthnüller, Comput. Mater. Sci. **6**, 15 (1996).
[24]P. E. Blöchl, Phys. Rev. B **50**, 17953 (1994).
[25]R. A. Webb, S. Washborn, C. P. Umbach, and R. B. Laibowitz, Phys. Rev. Lett. **54**, 2696 (1985).
[26]M. Bockrath, D. H. Cobden, P. L. Mceuren, N. G. Chopra, A. Zettl, A. Thess, and R. E. Smalley, Science **275**, 1922 (1997).
[27]C. Berger, P. Poncharal, Y. Yi, and W. De Heer, J. Nanosci. Nanotechnol. **3**, 171 (2003).
[28]M. Fukuhara, A. Kawashima, W. Zhang, and A. Inoue, J. Appl. Phys. **103**, 013503 (2008).
[29]M. Fukuhara, H. Yoshida, K. Koyama, A. Inoue, and Y. Miura, J. Nanosci. Nanotechnol. (in press).
[30]H. Oji, K. Handa, J. Ide, T. Honma, S. Yamaura, A. Inoue, N. Umesaki, S. Emura, and M. Fukuhara, J. Appl. Phys. **105**, 113527 (2009).
[31]H. Oji, K. Handa, J. Ide, T. Honma, N. Umesaki, S. Yamaura, M. Fukuhara, A. Inoue, and S. Emura, J. Phys.: Conf. Ser. **190**, 012075 (2009).
[32]J. Millman and S. Seely, *Electronics* (McGraw-Hill, New York, 1951).
[33]M. Fukuhara, M. Seto, and A. Inoue, Appl. Phys. Lett. **96**, 043103 (2010).
[34]H. W. Sheng, W. K. Luo, F. M. Alamgir, J. M. Bai, and E. Ma, Nature (London) **439**, 419 (2006).
[35]*International Tables for X-Ray Crystallography* (Kynoch, Birmingham, 1968), Vol. 3, p. 166.
[36]M. Fukuhara, Mol. Cryst. Liq. Cryst. **258**, 299 (1995).
[37]T. Fukunaga, K. Itoh, T. Otomo, K. Mori, M. Sugiyama, H. Kato, M. Hasegawa, A. Hirata, Y. Hirotsu, and A. C. Honnon, Mater. Trans. **48**, 1698 (2007).
[38]M. Fukuhara, Phys. Status Solidi B **175**, 421 (1993).
[39]T. Egami, Mater. Res. Bull. **13**, 557 (1978).